Supporting Information

Boosting the Efficient Urea Synthesis by the Cooperative Electroreduction of N₂ and CO₂ on MoP

Dongxu Jiao,[1,2,#,] Yilong Dong,[2, #,] Xiaoqiang Cui,[2,*] Qinghai Cai,[1,3]

Carlos R. Cabrera,[4] Jingxiang Zhao,[1,*] Zhongfang Chen[5,*]

[1] College of Chemistry and Chemical Engineering, and Key Laboratory of Photonic and Electronic Bandgap Materials, Ministry of Education, Harbin Normal University, Harbin 150025, China

[2] State Key Laboratory of Automotive Simulation and Control, School of Materials Science and Engineering, and Key Laboratory of Automobile Materials of MOE, Jilin University, Changchun 130012, China

[3] Heilongjiang Province Collaborative Innovation Center of Cold Region Ecological Safety, Harbin 150025, China

[4] Department of Chemistry and Biochemistry, The University of Texas at El Paso, El Paso, Texas 79968, USA

[5] Department of Chemistry, University of Puerto Rico, Rio Piedras Campus, San Juan, Puerto Rico 00931, USA

[*] To whom correspondence should be addressed. Email: *xjz_hmily@163.com (J.Z.);* *xqcui@jlu.edu.cn (X.C.); zhongfang.chen1@upr.edu (Z.C.)*

[#] *Dongxu Jiao and Yilong Dong contribute equally to this work.*

Materials

Thiosemicarbazide (CH_5N_3S, 99%), diacetyl monoxime ($C_4H_7NO_2$, >98%), and phosphoric acid (H_3PO_4 ≥85 wt. % in H_2O, ≥99.99% metal basis) were purchased from Shanghai Aladdin Biochemical Technology Co. Potassium bicarbonate ($KHCO_3$, AR), urea (CH_4N_2O, AR), iron (III) chloride anhydrous ($FeCl_3$, CP), and sulfuric acid (H_2SO_4, ≥85%) were obtained from Sinopharm Chemical Reagent (China). Ethanol (C_2H_5OH, AR) was obtained from Tianjin Fuyu Fine Chemical Co. Hydrophobic Carbon paper was received from Shanghai Hesen Electric Co., Ltd. (Shanghai, China). Nafion D-521 dispersion (5% w/w in water) was obtained from Alfa Aesar (China) Chemical Co. MoP was purchased from Shanghai Macklin Biochemical Co., Ltd. Argon (Ar, high purity 99.999%), carbon dioxide (CO_2 high purity 99.999%), nitrogen (N_2, high purity 99.999%), carbon dioxide and nitrogen mixed gas (CO_2 and N_2, high purity 99.999%) were obtained from Xin'guang Gas Co., China. All the chemicals were commercial and used without further purification. Ultrapure water (18.2 MΩ cm) was used in all experiments.

(a) **Mo-terminated**

side-view   top-view

(100)

P-terminated

side-view   top-view

(b) **Mo-terminated**

side-view   top-view

(001)

P-terminated

side-view   top-view
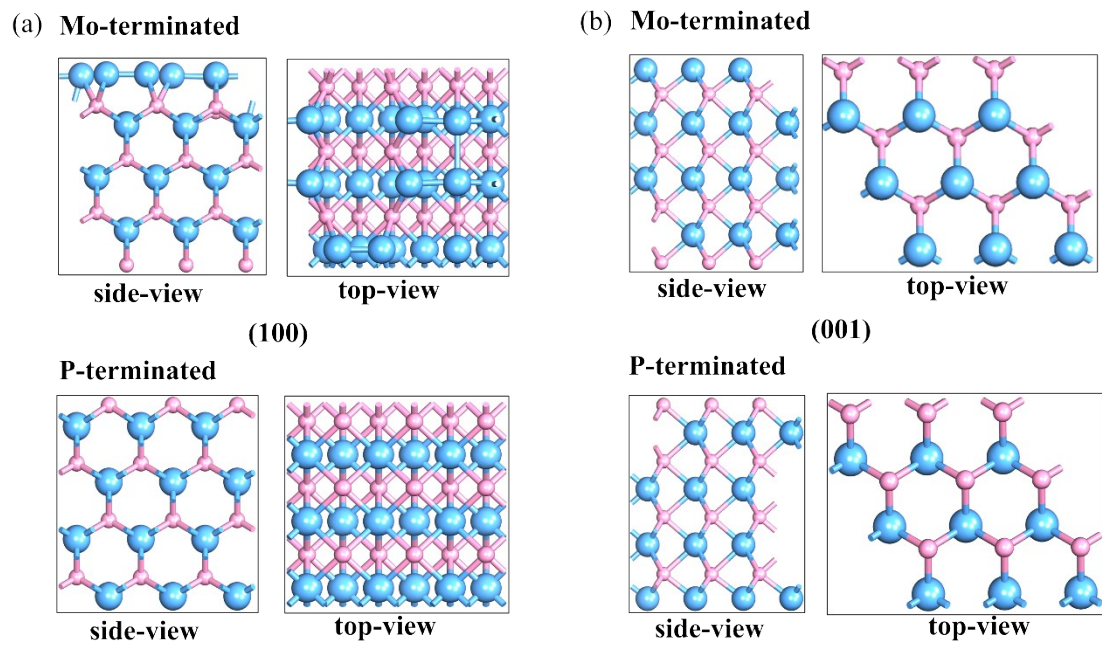
Fig. S1. The optimized geometric structures of (a) MoP-(100) surface and (b) MoP-(001) surface in MoP.
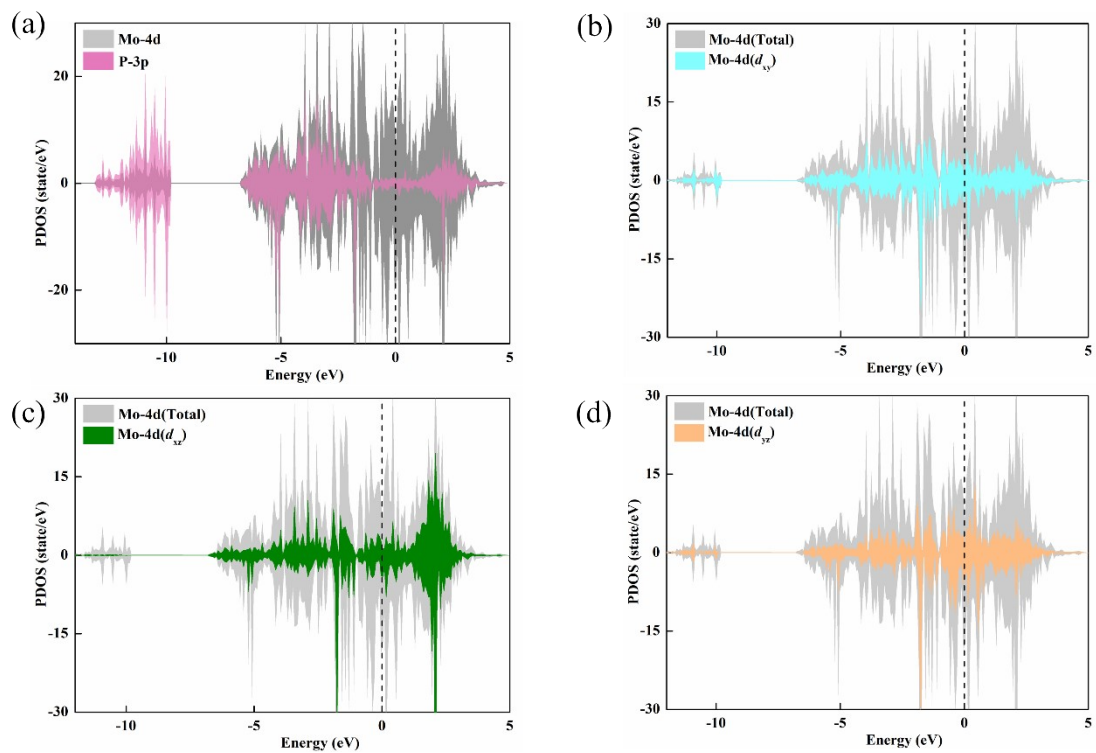
Fig. S2. The computed projected density of states (PDOSs) (a) Mo and P, (b) Mo-d_{xy}, (c) Mo-d_{xz}, and (d) Mo-d_{yz} of Mo-terminated MoP-(101) surface. The Fermi level was set as zero in dotted line.

Table S1. The computed free energy changes (ΔG, eV) of all possible elementary steps during urea synthesis on MoP-(101) surface. The ΔG values of the preferable steps are remarked in red.

Elementary step	ΔG
N_2 (g) $\rightarrow$ $^*N_2$	-0.43
$^*N_2 + CO_2 \rightarrow {}^*N_2 + {}^*CO_2$	-0.37
$^*N_2 + H^+ + e^- \rightarrow {}^*N_2H$	0.05
$^*N_2 + {}^*CO_2 + H^+ + e^- \rightarrow {}^*N_2 + {}^*COOH$	-0.51
$^*N_2 + {}^*CO_2 + H^+ + e^- \rightarrow {}^*N_2H + {}^*CO_2$	-0.06
$^*N_2 + {}^*COOH + H^+ + e^- \rightarrow {}^*N_2 + {}^*CO + H_2O$	0.17
$^*N_2 + {}^*COOH + H^+ + e^- \rightarrow {}^*N_2H + {}^*COOH$	0.21
$^*N_2 + {}^*CO + H^+ + e^- \rightarrow {}^*N_2H + {}^*CO$	0.09
$^*N_2 + {}^*CO \rightarrow {}^*NCON$	0.48
$^*N_2 + {}^*CO + H^+ + e^- \rightarrow {}^*N_2H + {}^*COH$	1.34
$^*N_2 + {}^*CO + H^+ + e^- \rightarrow {}^*N_2H + {}^*CHO$	0.91
$^*N_2H + {}^*CO + H^+ + e^- \rightarrow {}^*HNNH + {}^*CO$	-0.16
$^*N_2H + {}^*CO \rightarrow {}^*NCONH$	-0.06
$^*N_2H + {}^*CO + H^+ + e^- \rightarrow {}^*N_2H + {}^*COH$	1.41
$^*N_2H + {}^*CO + H^+ + e^- \rightarrow {}^*N_2H + {}^*CHO$	0.94
$^*N_2H + {}^*CO + H^+ + e^- \rightarrow {}^*NNH_2 + {}^*CO$	0.35
$^*HNNH + {}^*CO \rightarrow {}^*NHCONH$	-0.25
$^*HNNH + {}^*CO + H^+ + e^- \rightarrow {}^*HNNH_2 + {}^*CO$	0.16
$^*HNNH + {}^*CO + H^+ + e^- \rightarrow {}^*HNNH + {}^*COH$	1.45
$^*HNNH + {}^*CO + H^+ + e^- \rightarrow {}^*HNNH + {}^*CHO$	0.98
$^*NHCONH + H^+ + e^- \rightarrow {}^*NH_2CONH$	0.27
$^*NHCONH + H^+ + e^- \rightarrow {}^*NHCOHNH$	0.34
$^*NH_2CONH + H^+ + e^- \rightarrow {}^*urea$	0.25
$^*NH_2CONH + H^+ + e^- \rightarrow {}^*NH_2COHNH$	0.65
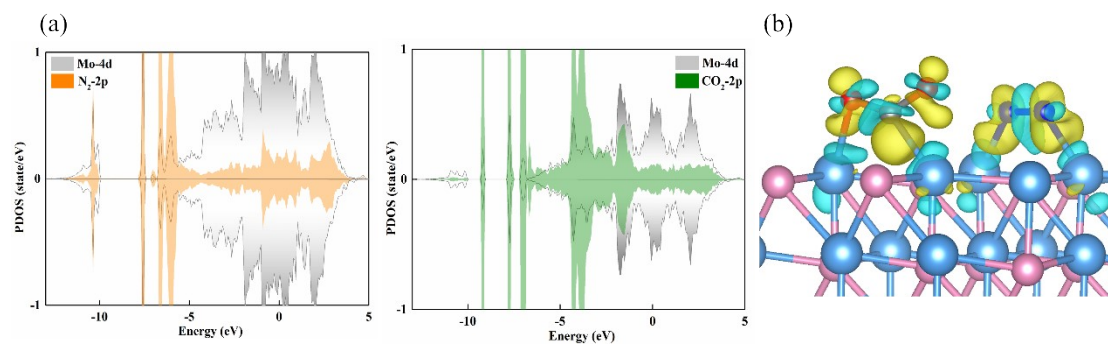
Fig. S3. The computed PDOS (a) of N_2 and CO_2 adsorption on MoP-(101) surface and (b) charge density difference. The iso-surface value was set to be 0.005 $e/\text{Å}^3$ and the positive and negative charges are shown in cyan and yellow, respectively.
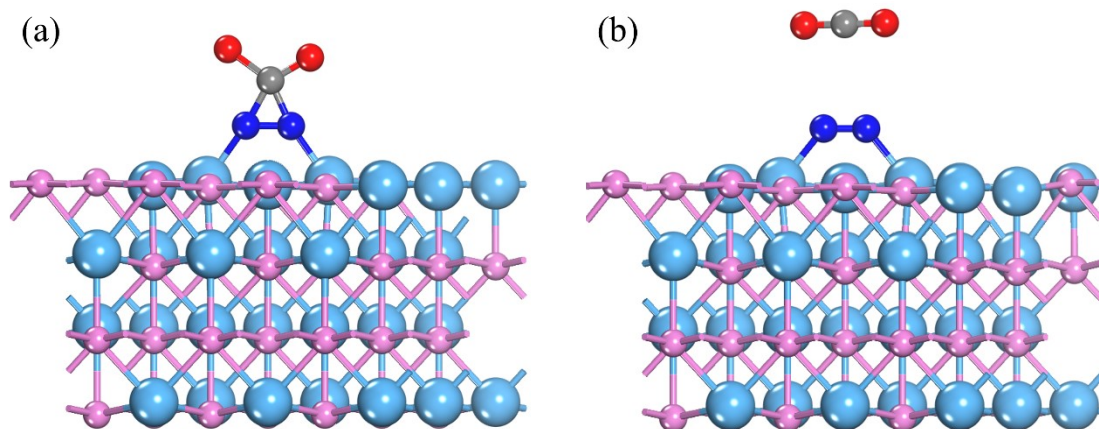
Fig. S4. The structure of CO_2 and N_2 coupling (a) before structural optimization, (b) after structure optimization.
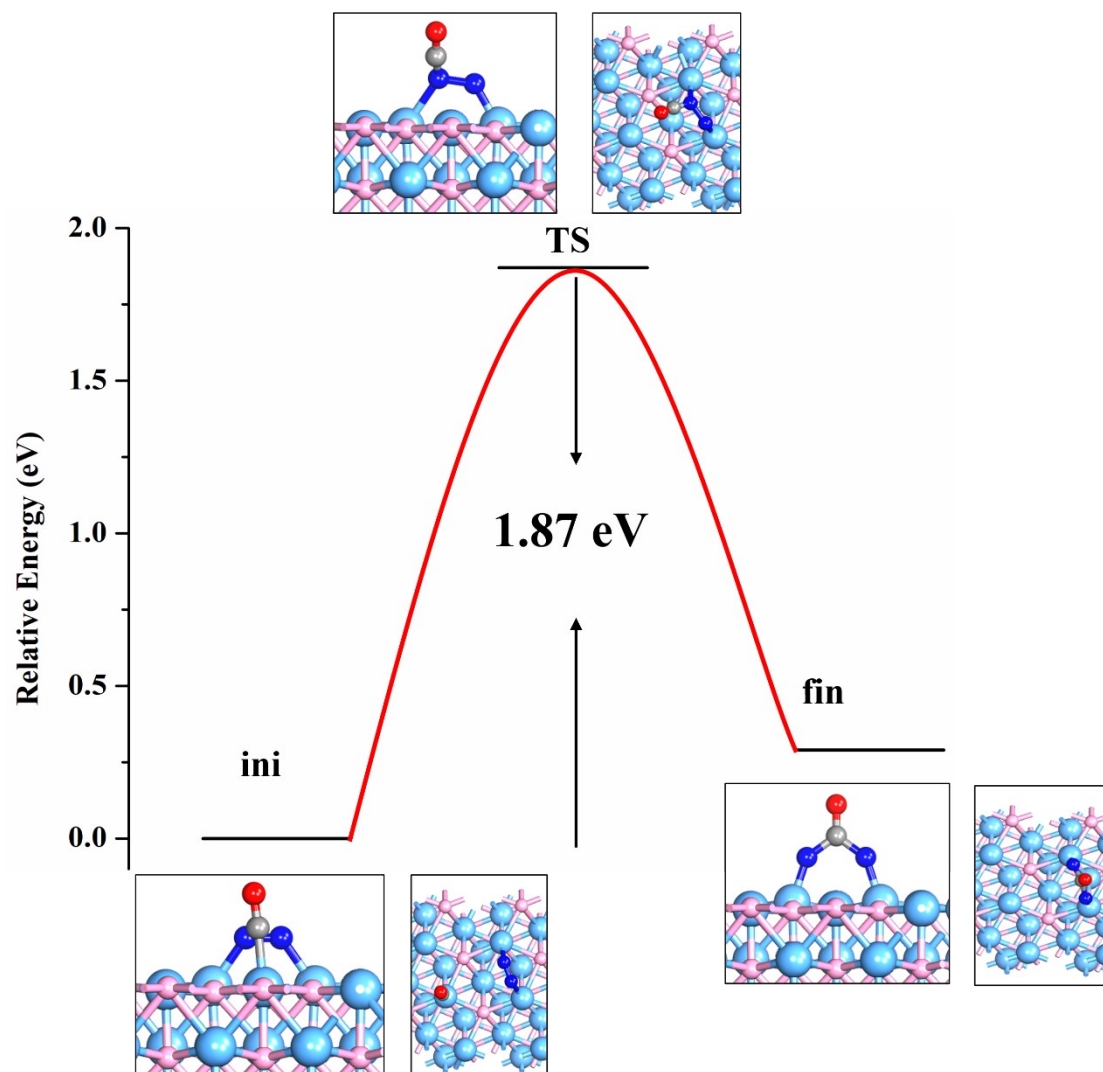
Fig. S5. The computed pathway for C–N coupling reaction between $^*CO$ and $^*N_2$ on the MoP-(101) surface. ini, TS, and fin represent the initial state, transition state, and final state, respectively.
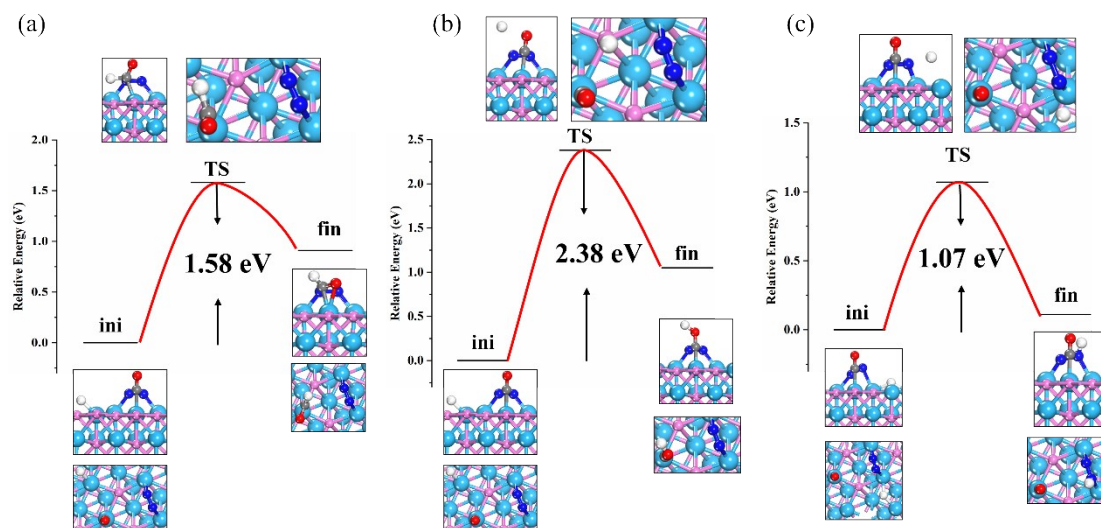
Fig. S6. The computed pathway of the CO + N_2 coupling reaction to form (a) $^*N_2$ + $^*CHO$, (b) $^*N_2$ + $^*COH$, and (c) $^*N_2H$ + $^*CO$ on the MoP-(101) surface. ini, TS, and fin represent the initial state, transition state, and final state, respectively.
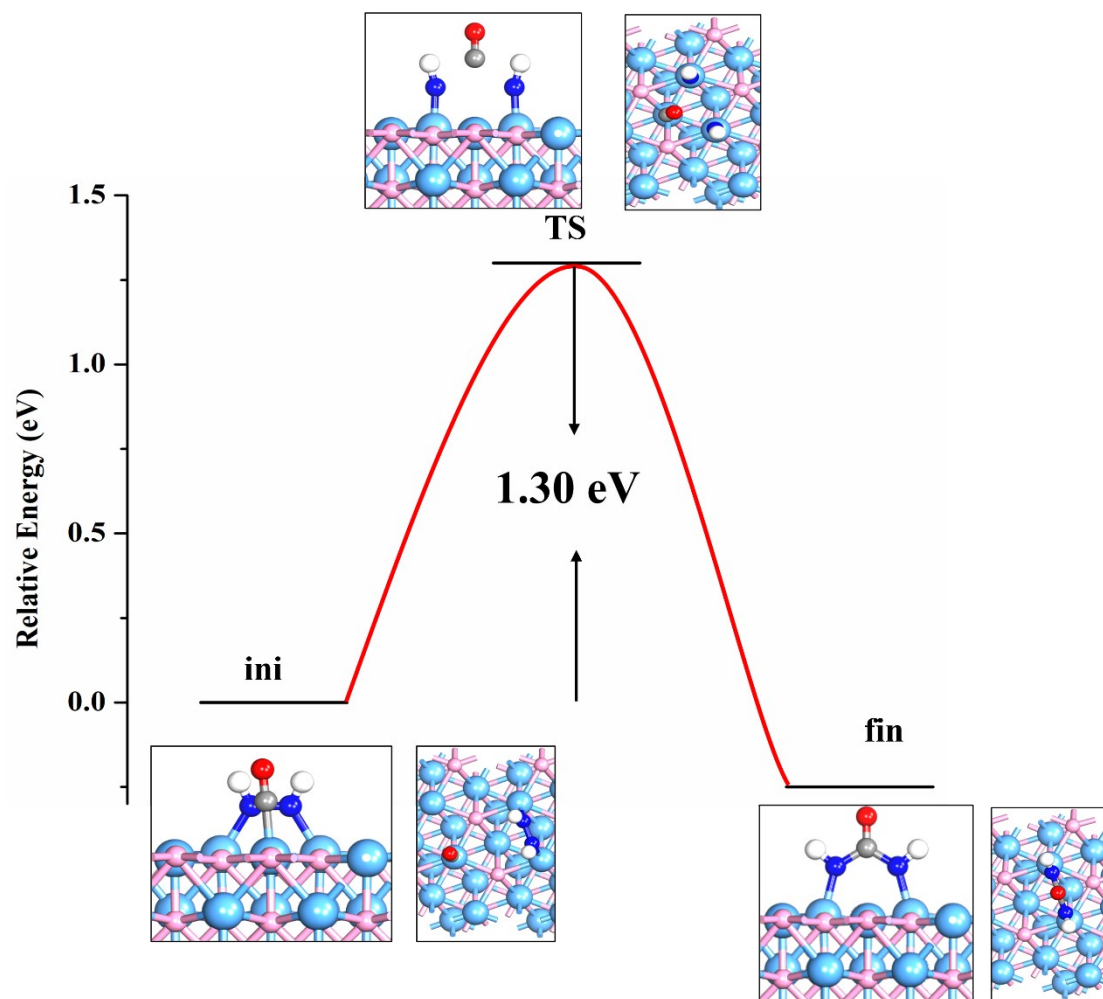
Fig. S7. The computed pathway for the C–N coupling reaction between *CO and *HNNH on the MoP-(101) surface. ini, TS, and fin represent the initial state, transition state, and final state, respectively.
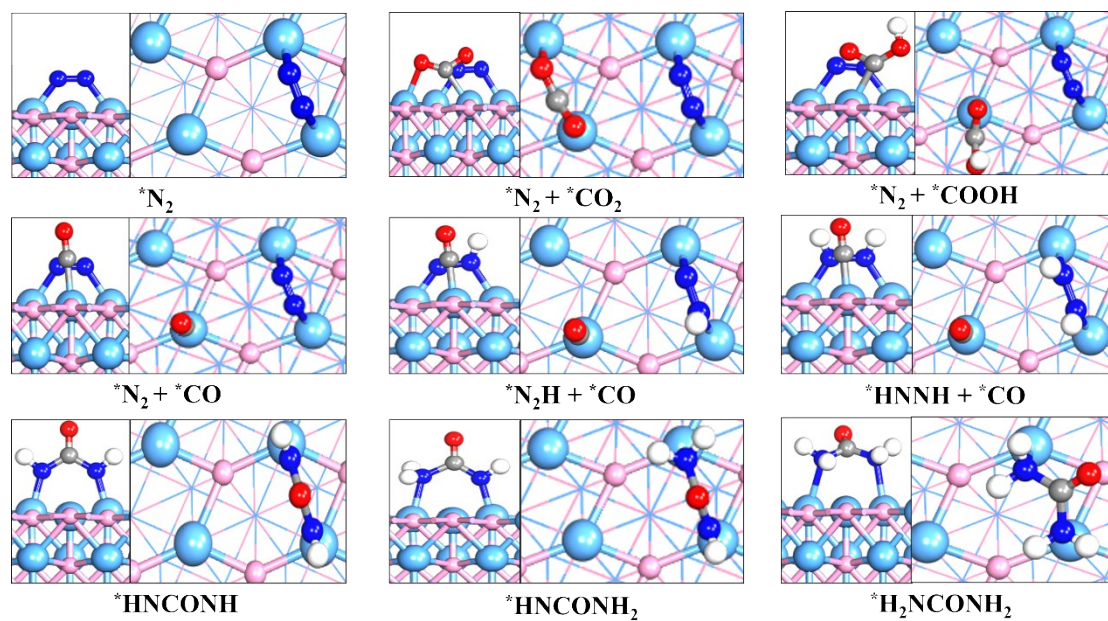
Fig. S8. The involved intermediates during urea synthesis on MoP-(101) surface.
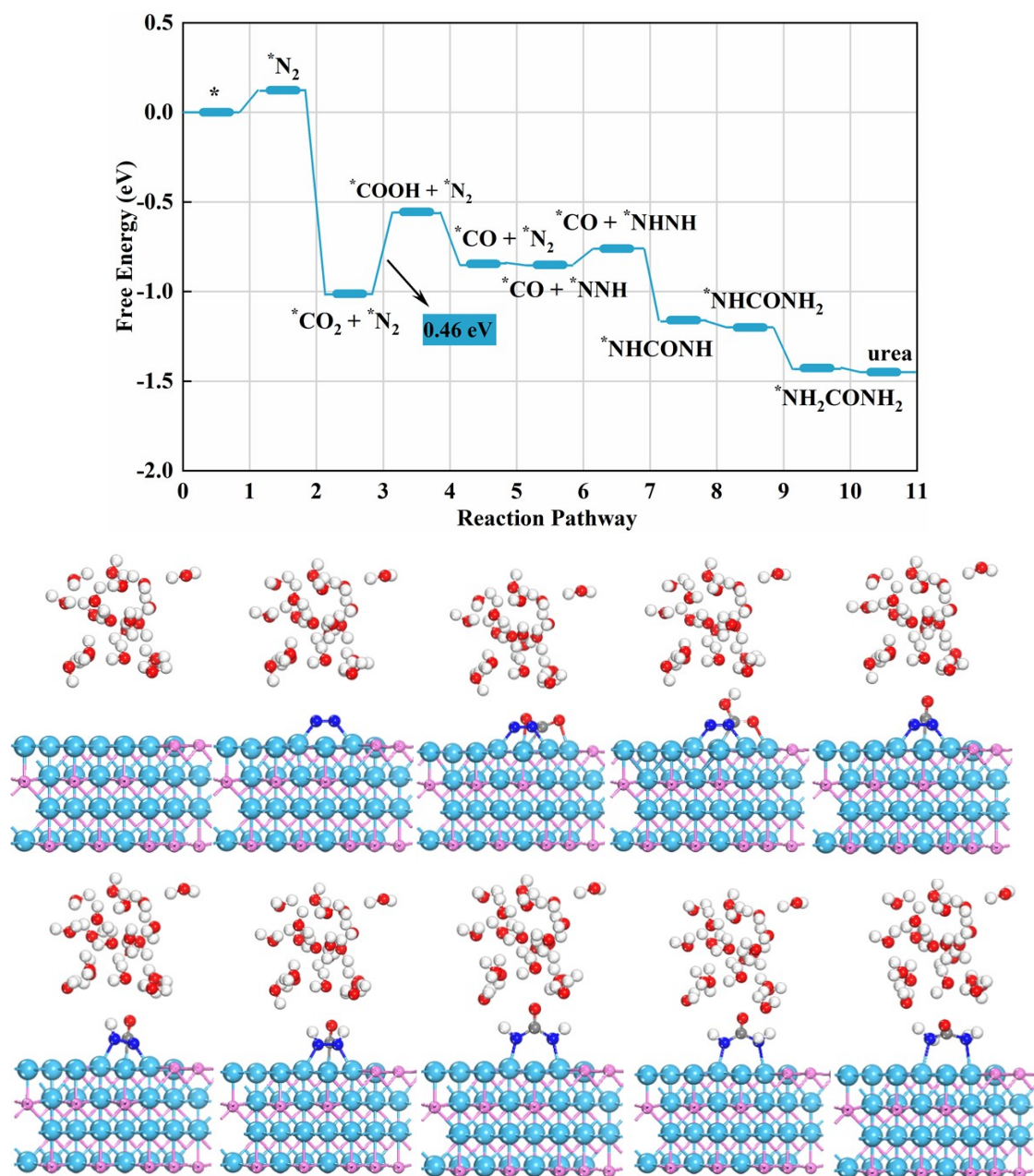
Fig. S9. The computed free energy profiles and corresponding structure diagram for MoP-(101) after considering the explicit solvent model.
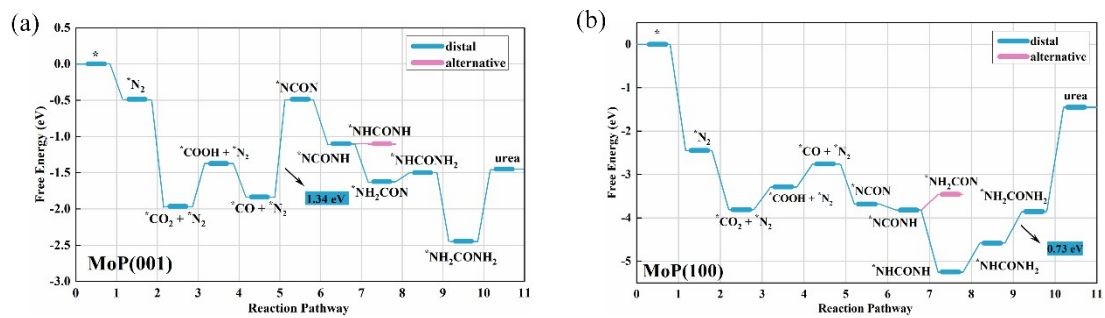
Fig. S10. The computed free energy profiles for (a) MoP-(001) and (b) MoP-(100) surface.
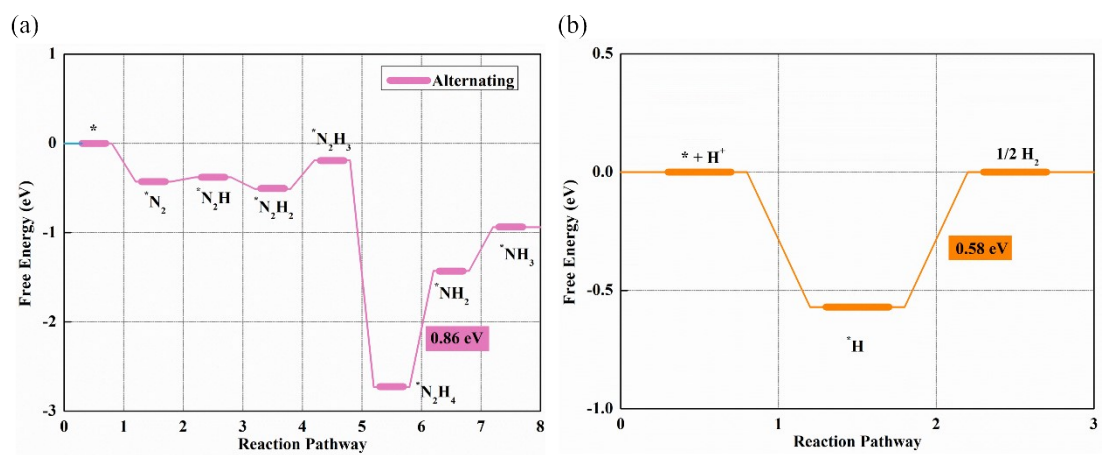
Fig. S11. The computed free energy profiles for NRR on the MoP-(101) surface.
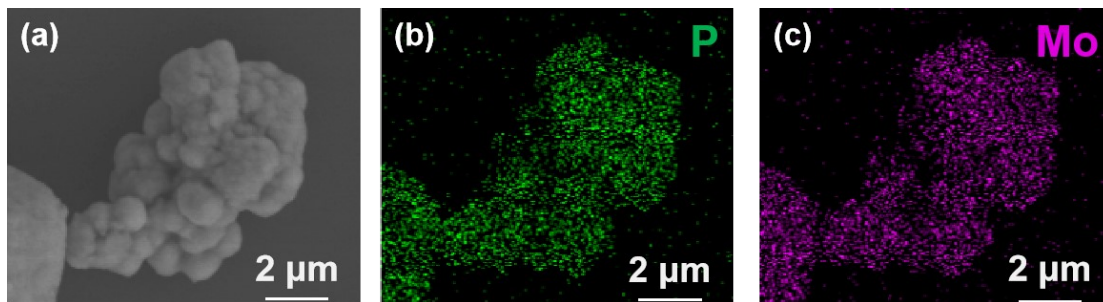
Fig. S12. SEM image (a), and the EDX elemental mapping of MoP nanoparticles: P (b) and Mo (c).
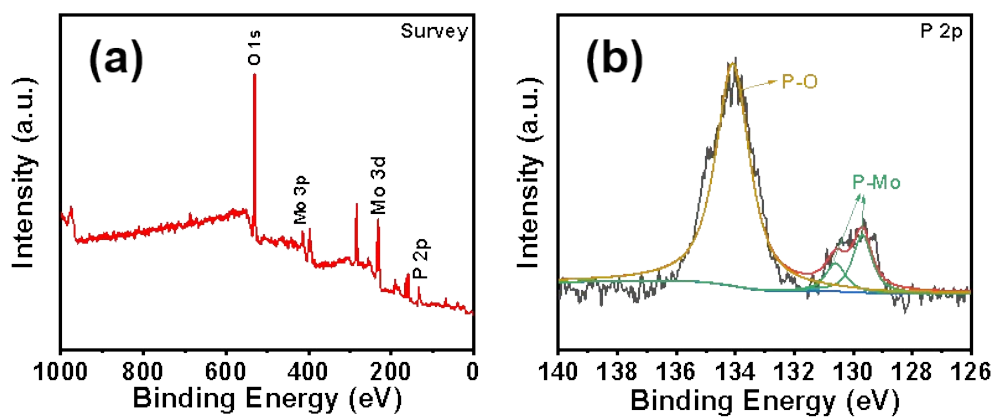
Fig. S13. (a)Wide-scan survey XPS spectrum of MoP and (b) XPS spectra of P 2p of MoP.
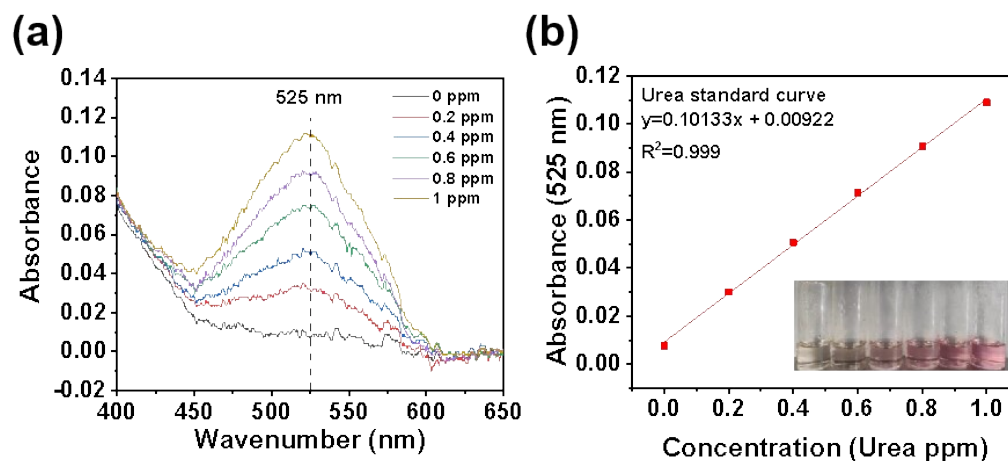
Fig. S14. (a) UV-vis curves and (b) concentration-absorbance of urea solution with a series of standard concentration (0-1.0 μg mL^{-1}) in 0.1M KHCO$_3$. The absorbance at 525 nm was measures by UV-vis spectrophotometer. The standard curve showed a good linear relation of absorbance with urea concentration (y=0.10133x+0.00922, R^2=0.999), the standard curve was derived from three independent replicate experiments to ensure its accuracy.
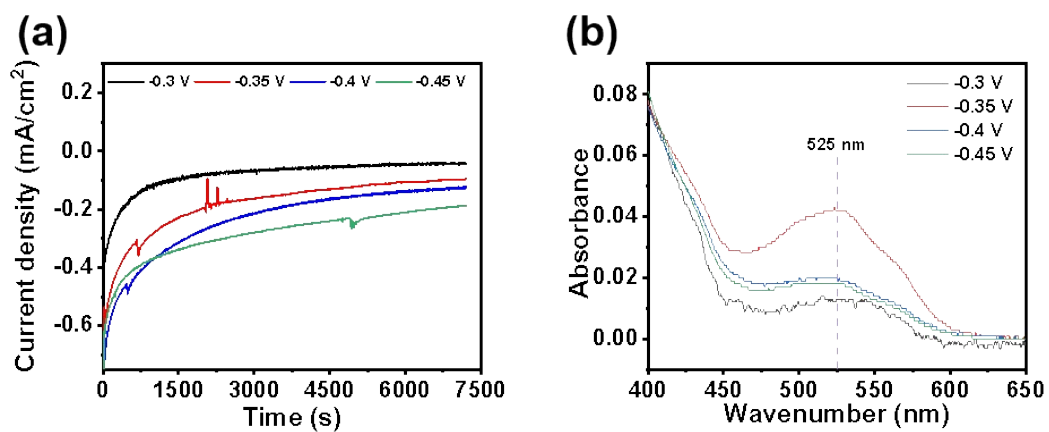
Fig. S15. (a) Chronoamperometric curves of MoP catalysts in 0.1M $KHCO_3$ solution at different working potentials for 2h. (b) UV-vis absorbance spectra of the electrolyte after the electrochemical reaction.

Table S2. Comparison of urea yield rate and FEs among MoP and other reported urea synthesis electrocatalysts.

Catalysts	Urea yield	Faradaic Efficiency
MoP (This Work)	12.4 μg h^{-1} mg$^{-1}_{cat}$	36.5%
Cu-Pc	143.47 μg h^{-1} mg$^{-1}_{cat}$	12.99%
Cu-Pd alloy	3.36 mmol g^{-1} h^{-1}	8.92%
Ni$_3$(BO$_3$)$_2$	9.70 mmol h^{-1} g$_{cat}^{-1}$	20.36%
Bi-BiVO$_4$	5.91 mmol h^{-1} g^{-1}	12.55%
InOOH	6.85 mmol h^{-1} g^{-1}	20.97%
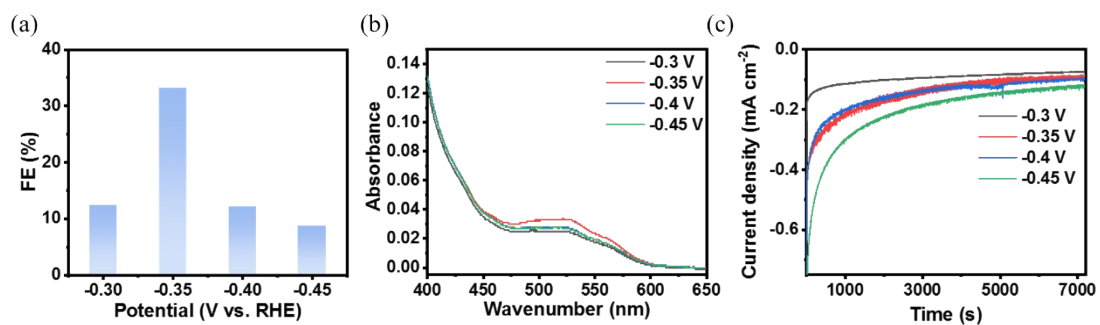
Fig. S16. (a) Faradaic efficiencies of urea at the different working potentials for MoP, (b) the UV-vis curves and (c) Chronoamperometric curves of MoP catalysts in 0.1M KHCO$_3$ solution at the different working potentials for 2h. The MoP from Aladdin.

(a)

(b)
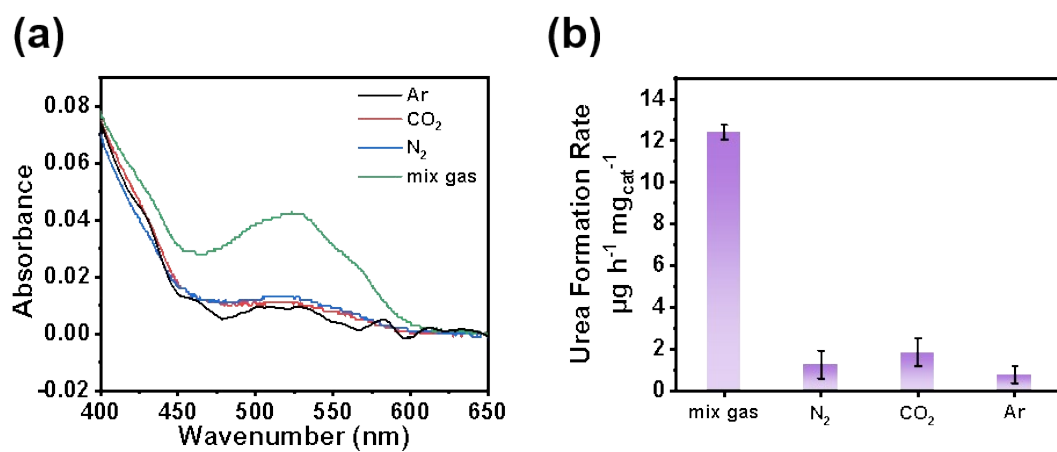
Fig. S17. (a) The UV-vis curves and (b) the urea formation rate of MoP catalyst at -

0.35 V vs. RHE with different feeding gas.
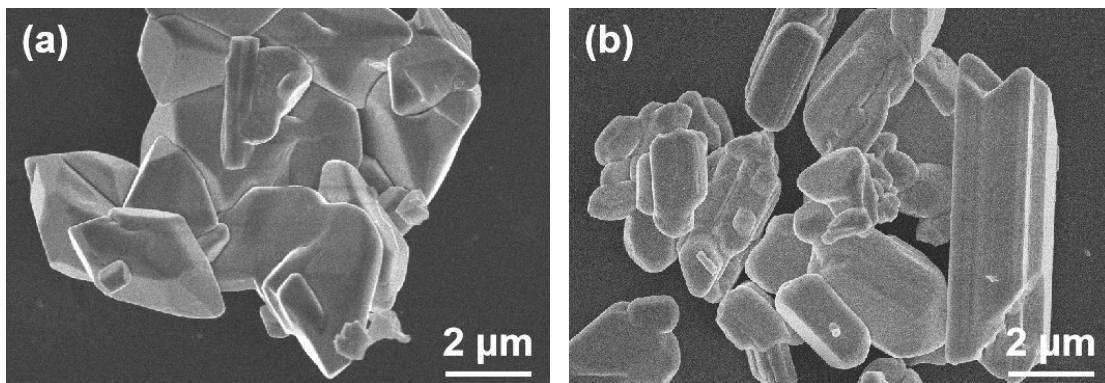
Fig. S18. SEM images of (a) MoO_2, (b) MoO_3 nanoparticles.
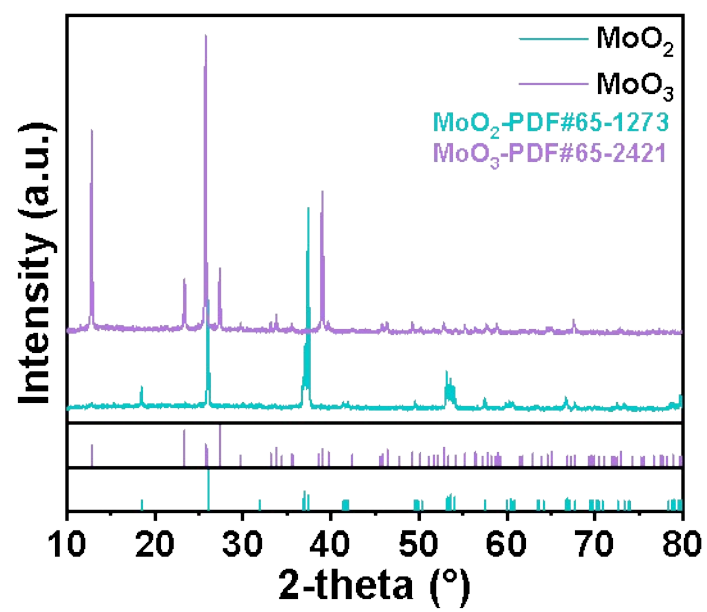
Fig. S19. XRD pattern of MoO_2 and MoO_3 nanoparticles.
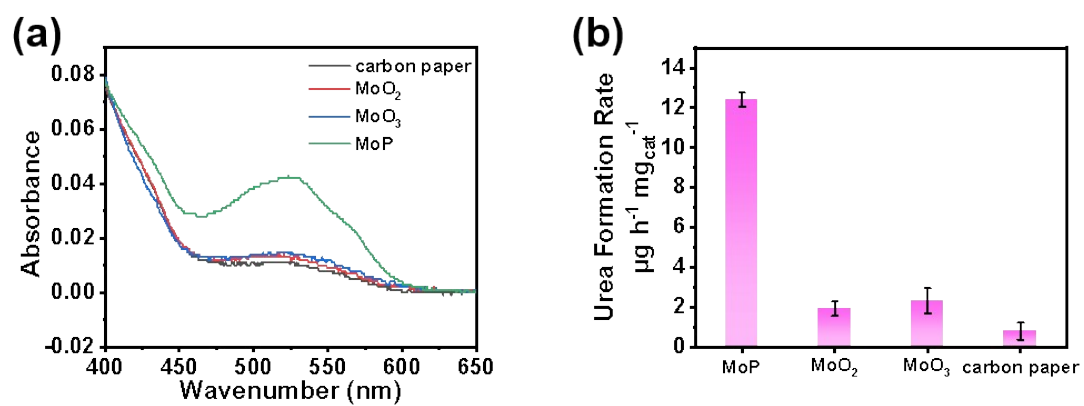
Fig. S20. (a) The UV-vis curves and (b) the urea formation rate of different electrodes at -0.35 V vs. RHE using mixed CO_2 and N_2 as feeding gas.
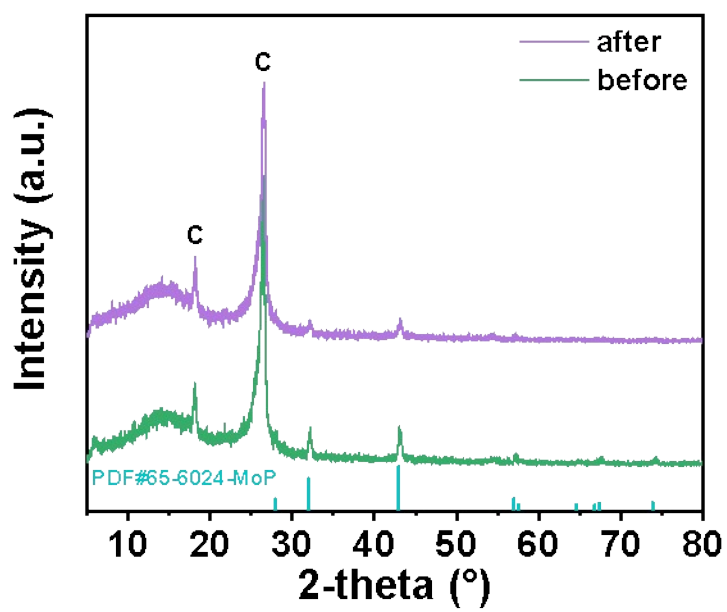
Fig. S21. XRD pattern of the MoP dropped in carbon paper and that of the same

sample after 2 h electroreduction.
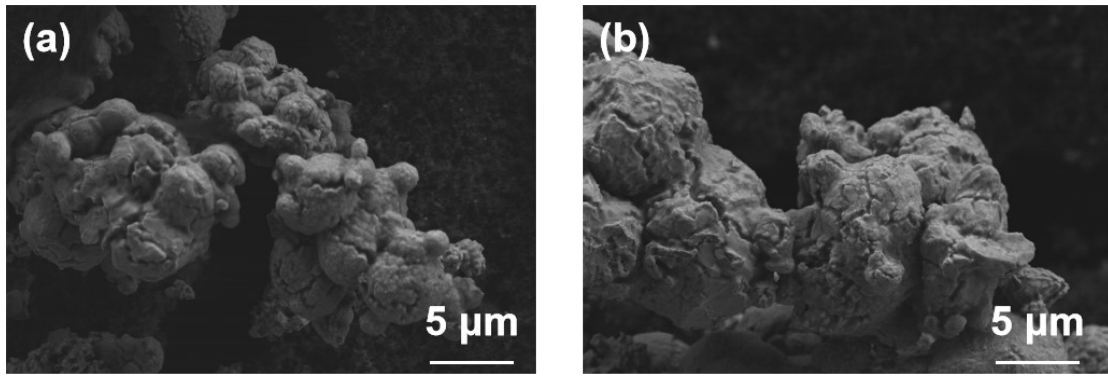
Fig. S22. (a) SEM image of the MoP dropped in carbon paper and (b) SEM image of the same sample after 2 h electroreduction.
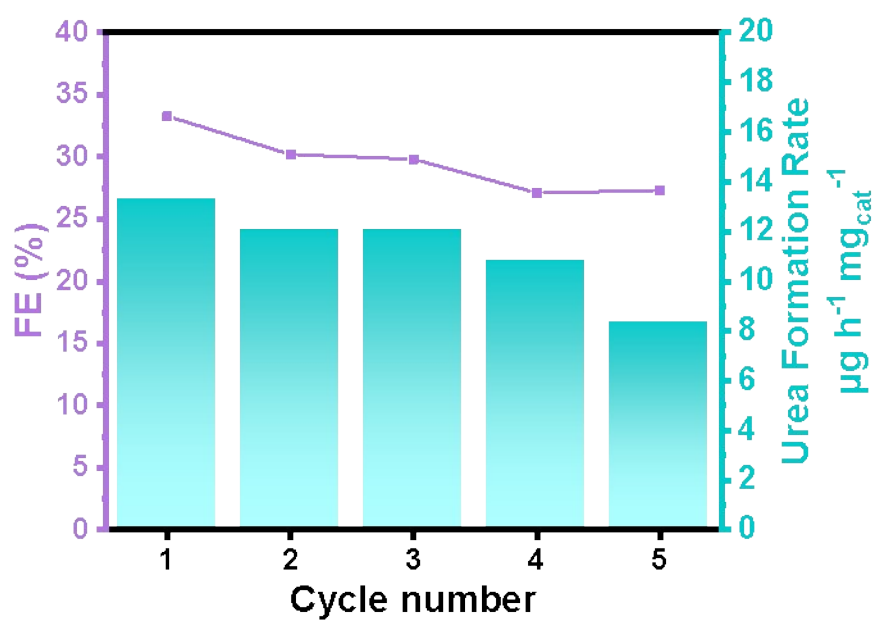
Fig. S23. The FE and urea formation rate of MoP catalyst at -0.35 V vs. RHE during recycling tests for five times.
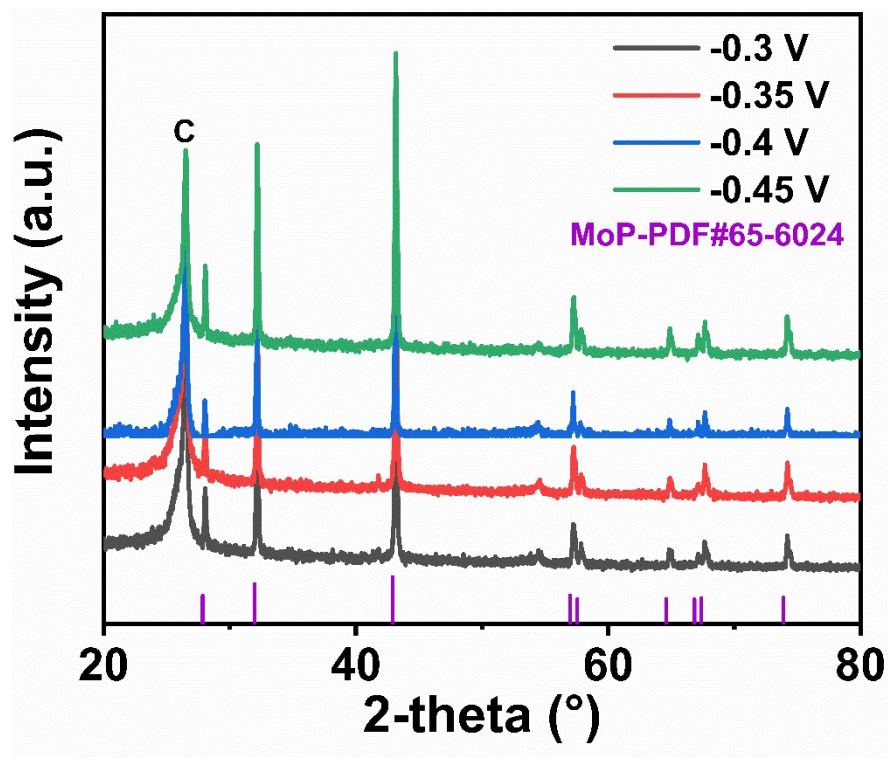
Fig. S24. XRD pattern of the MoP dropped in carbon paper at different potentials.
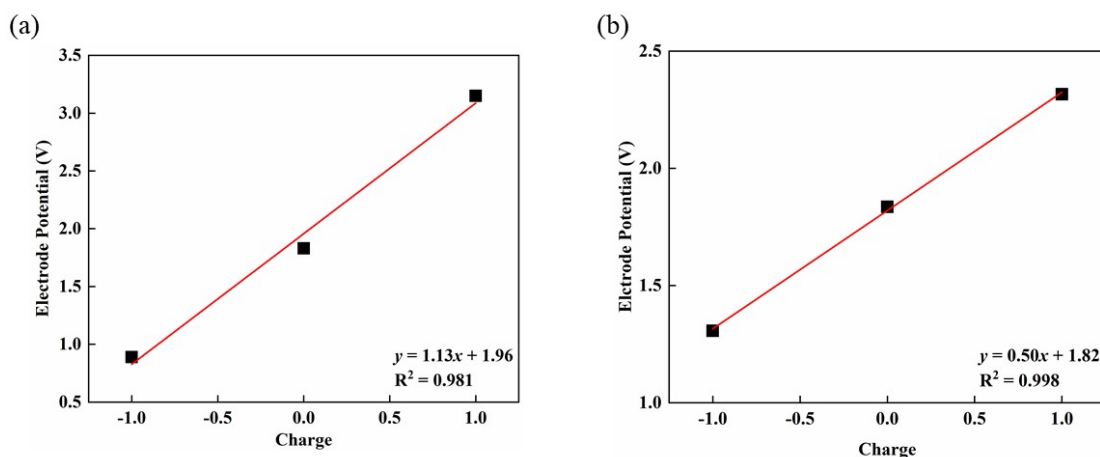
Fig. S25. Electrode potential calculated from the workfunction of (a) MoP-(101) and (b) N_2 and CO_2 adsorption on MoP-(101) models with different number of electrons, with adsorbate in presence.

The relationship between electrode potential and work function of the electrode is:

$$U = (W_f - 4.6)/eV + 0.0592 \times pH \quad (1)$$

Where U is the electrode potential, W_f is the work function, 4.6 eV is the work function of the normal hydrogen electrode (NHE), and 0.0592 is the potential change by one pH unit. In this study, we set the pH = 0. Thus, the W_f at targeted U can be derived with equation 1. We then carried out electrode potential calculations at different charged states for MoP-(101), and extrapolated the electron number e^- for the electrode potential.